Biosensors and Bioelectronics 26 (2010) 365–370

Contents lists available at ScienceDirect

Biosensors and Bioelectronics

journal homepage: www.elsevier.com/locate/bios

Highly sensitive and reversible silicon nanowire biosensor to study nuclear hormone receptor protein and response element DNA interactions

Guo-Jun Zhang[a,*], Min Joon Huang[a], Zhan Hong Henry Luo[a], Guang Kai Ignatius Tay[a], Eu-Jin Andy Lim[a], Edison T. Liu[b], Jane S. Thomsen[b]

[a] Institute of Microelectronics, A*STAR (Agency for Science, Technology and Research), 11 Science Park Road, Singapore Science Park II, Singapore 117685, Singapore
[b] Genome Institute of Singapore, ASTAR (Agency for Science, Technology and Research), 60 Biopolis Street, Singapore 138672, Singapore

ARTICLE INFO

Article history:
Received 8 June 2010
Received in revised form 27 July 2010
Accepted 30 July 2010
Available online 6 August 2010

Keywords:
Silicon nanowire
Biosensor
Surface functionalization
Interactions
Protein
DNA

ABSTRACT

To thoroughly understand the role that estrogen receptors partake in regulation of gene expression, characterization of estrogen receptors (ERs) and estrogen-response elements (EREs) interactions is essential. In the work, we present a highly sensitive and reusable silicon nanowire (SiNW) biosensor to study the interactions between human ER proteins (ER, α and β subtypes) and EREs (dsDNA). The proteins were covalently immobilized on the SiNW surface. Various EREs including wild-type, mutant and scrambled DNA sequences were then applied to the protein-functionalized SiNW surface. Due to negatively charged dsDNA, binding of the EREs to the ERs on the n-type SiNW biosensor leads to the accumulation of negative charges on the surface, thereby inducing increase in resistance. The results show that the specificity of the ERE–ERα binding is higher than that of the ERE–ERβ binding, what is more, the mutant ERE reduces the binding affinity for both ERα and ERβ. By applying various concentrations of wild-type ERE to the bound ERα, a very low concentration of 10 fM wild-type ERE was found to be able to bind to the ERα. The reversible association and dissociation between ERα and wt-ERE was achieved, pointing to a reusable biosensor for protein–DNA binding. Through the study, we have established the SiNW biosensor as a promising method in providing comprehensive study for hormone receptor–response element interactions.

1. Introduction

Estrogen receptors (ERs) are members of a superfamily of nuclear receptors that function as ligand-modulated transcriptional regulators (Evans, 1988; Moras and Gronemeyer, 1998). The ERs mainly function as a DNA binding transcription factor that regulates gene expression. They play a key role in many normal physiological processes, but promote aberrant growth of breast cancer cells. Ligand-activated ERs directly bind to specific DNA sequences known as estrogen-response elements (EREs) present in estrogen-sensitive gene promoters. The sequence of all known EREs is based on a perfect inverted repeat separated by a three-base spacer, 5′-GGTCAnnnTGACC-3′ (Klein-Hitpass et al., 1986, 1988). However, many naturally occurring estrogen-responsive genes have two or more imperfect core consensus sequences. As a result, a sensitive solution to differentiate between subtle differences in ER–DNA binding affinities is highly desirable.

The interactions of ER with an ERE have been analyzed mainly by conventional techniques like electrophoretic mobility shift assay (EMSA) (Loven et al., 2001; Yi et al., 2002), DNA foot-printing (Driscoll et al., 1996), and fluorescence anisotropy (Ozers et al., 1997). However, these methods involve labeling and long incubation period, which are not suitable for the analysis of large kinds of samples, or small amount of samples. A novel method of on-chip detection of ERα and DNA interactions at single molecular level using atomic force microscopy (AFM) has been reported (Lyubchenko and Shlyakhtenko, 2009; Wicaksono et al., 2004). AFM usually requires skillful technicians to manipulate. Moreover, the most serious disadvantage of the AFM is its relatively slow image acquisition. ER–ERE interactions using surface plasmon resonance (SPR) methodology were analyzed in real-time, demonstrating that ligand binding dramatically affects the kinetics of hER interaction with specific DNA (Cheskis et al., 1997). Very recently, combination of SPR and quartz crystal microbalance (QCM) has been introduced to characterize the interactions of ER and ERE (Su et al., 2006; Teh et al., 2007). The method allows real-time, label-free monitoring of biomolecular interactions. Nevertheless, the sensitivity obtained by the method is not satisfactory to study binding affinity of ER and various EREs, especially interactions of ER and the mutant EREs which contain base substitution in ERE half-sites.

Silicon nanowires (SiNWs) biosensor is a recently developed technology, which is capable of label-free and highly sensitive

* Corresponding author. Tel.: +65 6770 5390, fax: +65 6774 5754.
E-mail address: zhanggj@ime.a-star.edu.sg (G.-J. Zhang).

0956-5663/$ – see front matter © 2010 Elsevier B.V. All rights reserved.
doi:10.1016/j.bios.2010.07.129

detection of biomolecules such as nucleic acids (Bunimovich et al., 2006; Gao et al., 2007; Hahm and Lieber, 2004; Li et al., 2004; Zhang et al., 2008a,b, 2009, 2010) and proteins (Chua et al., 2009; Cui et al., 2001; Lin et al., 2010; Stern et al., 2007a; Zheng et al., 2005). In most cases, protein detection was carried out using the antibody-functionalized SiNW biosensor. The applications include detection of various biomarkers with the approach. On the other hand, peptide nucleic acid (PNA)-functionalized SiNW biosensor was used to detect DNA and microRNA. Furthermore, the PNA-functionalized SiNW biosensors were able to distinguish single base mutation. Although the SiNW biosensor has been intensively explored, little, to date, is known about studying protein–DNA interactions using the SiNW biosensor.

In the study, we, for the first time, characterized the interactions between ERs (ER, α and β subtypes) and EREs by using the highly sensitive and label-free electrical SiNW biosensor platform. Different from the previously reported methods in which ERE was immobilized on the sensor surface, we covalently immobilized ER on the SiNW surface and bound the ERE to the ER-functionalized SiNW. Because the ERE is double-stranded DNA and each ERE contains 50 negative charges in the study (25 bp for both reverse and forward sequences), this detection scheme facilitates accumulation of more negative charges on the surface, thereby increasing the detection sensitivity. In order to understand the sensing behavior, various studies including specificity of ER–ERE binding, limit of detection, influence of buffer ionic strength on incubation and on detection, respectively, were conducted. Moreover, the studies on the association and dissociation of ER–ERE binding were also carried out. With this study, the SiNW biosensor has been developed as a potential approach to providing a comprehensive study for hormone receptor protein–response element DNA interactions.

2. Materials and methods

2.1. Materials

Chemicals that were involved in the surface modification procedure, namely aminopropyltriethoxysilane (APTES), glutaraldehyde and O-(2-aminoethyl)-O′-methylpolyethyleneglycol 750 (amino-PEG) were purchased from Sigma. Two forms of human recombinant ERs, ERα and ERβ, were purchased from Invitrogen. 25-bp ERE sequences, wild-type ERE (wt-ERE) which possesses a consensus sequence with the palindromic GGTCA half-site, mutant ERE (mut-ERE) which possesses two base-pair mismatched with one base mismatch in each of the half-sites, and scrambled ERE sequence (non-ERE), which contains the same genetic makeup as consensus sequence but in scrambled form to keep the CG content similar, were synthesized from Sigma–Aldrich. Table 1 shows the sequences of the three kinds of DNA.

2.2. SiNW fabrication

The SiNW biosensor was fabricated using the previously reported method (Zhang et al., 2010). Briefly, the SiNW sensor was prepared by self-limiting oxidation process of silicon beams patterned using conventional deep UV photolithography, which is electrically addressable on an individual basis.

Table 1
Sequences of EREs (DNA) employed in this study.

Name	Sequence
Wild-type ERE (wt-ERE)	5′-CAACTGGGTCATTCTGACCTAGAAG-3′
Mutant ERE (mut-ERE)	5′-CAACTGG*T*TCATTCTGA*T*CTAGGAAG-3′
Scrambled ERE (non-ERE)	5′-CAACTGATCGGTTCCTCGATAGAAG-3′

2.3. Annealing of EREs

As double-stranded ERE sequences act as the binding target in this work, annealing of EREs containing oligonucleotides in saline sodium citrate (SSC) buffer was necessary. To anneal the oligonucleotides, equal molar of complementary oligonucleotides, diluted to the required concentration by SSC buffer, were mixed together in an eppendorf tube and heated in a hot water bath (∼100 °C) for 5 min using a hotplate. The mixture was then removed from the hotplate and left to cool to room temperature gradually. Influence of salt concentration on the detection was explored by annealing the oligonucleotides of the intended concentration using SSC buffer of different ionic strengths.

2.4. Surface modification of SiNWs

Two-step conventional silane chemistry employed in this experiment was described previously (Chua et al., 2009; Zhang et al., 2010). The SiNW surface was first functionalized using APTES, followed by glutaraldehyde. This bifunctional linker constitutes of two aldehyde terminals, which enables one end binding to the amine-terminated APTES and the other end free to immobilize the ER protein. After which, an acrylic well was pasted onto the chip to enclose the area where SiNWs resided for localizing application of analytes. Following that, the ER protein was covalently bound onto the SiNW by applying 10 μl of ER analyte directly into the acrylic well. Incubation was achieved in a moist environment for 2 h. The unbounded ER proteins were then washed away using 1× PBS buffer. The ER-functionalized surface was then passivated with 1 mg/ml amino-PEG to minimize the unspecific binding.

2.5. Binding of ER with ERE

10 μl of the targeted ERE was applied onto the SiNW surface which was functionalized with ER, and the chip was incubated for 1 h in a moist environment. After incubation, excess ERE targets were washed away with 1× SSC.

2.6. Electrical measurement

The basic sensing mechanism was performed by observing the resistance change before and after binding of the ERE to the ER immobilized on the SiNW surface. In an ER–ERE binding event, an influx of negative charges, contributed by the negatively charged backbone of the dsDNA, would result in depletion within the SiNW bulk, leading to a decrease in conductance and in turn an increase in resistance (Zhang et al., 2008a,b, 2009, 2010). To verify this resistance change, resistance was being measured twice: before and after the addition of the ERE target. Thus, following the immobilization of the ER, resistances of 15 SiNW wires were measured by probing the two terminals, source (S) and drain (D) electrodes, with Alessi REL-6100 probe station (Cascade Microtech, Beaverton), in the presence of 0.01× SSC buffer solution. After ER–ERE binding, this bound complex was sent for a second electrical measurement. The resultant change in resistance was analyzed by using the formula $[(R - R_0)/R_0] \times 100$. The measurement was conducted according to the protocol described previously (Zhang et al., 2010).

3. Results and discussion

3.1. Working principle of SiNW biosensor for studying ER–ERE binding

The n-type SiNWs used in the work were produced using a top-down CMOS wafer fabrication based technique as described before

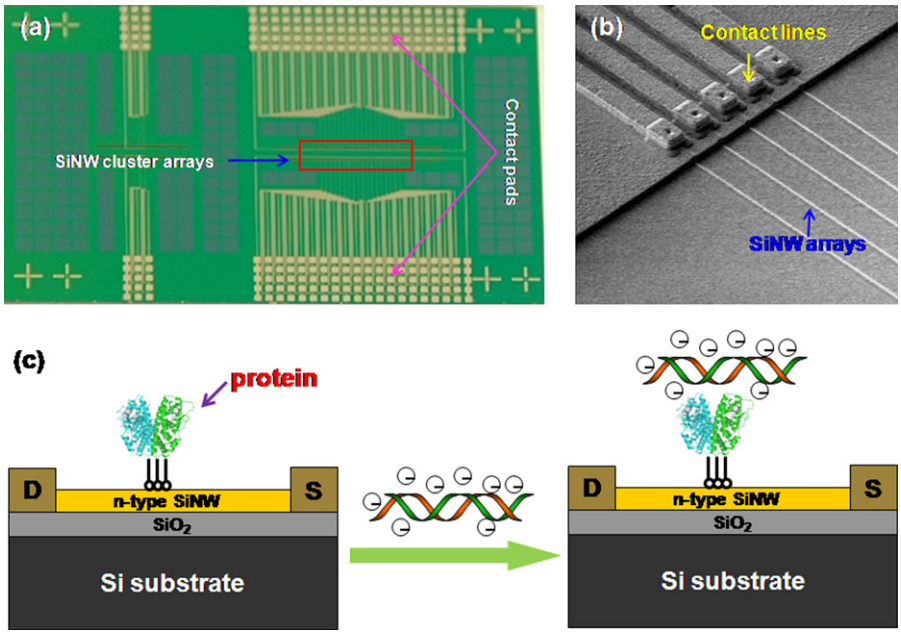

Fig. 1. (a) Optical image of SiNW array sensor chip. (b) SEM image of one cluster having 5 individual SiNW array sensors. (c) Schematic illustration of interactions of ER–ERE studied by the SiNW biosensor. ER is covalently immobilized on the SiNW surface, and ERE is bound to the specific ER. The ERE brings intrinsic negative charges to the SiNW surface, giving rise to increase in resistance in the n-type SiNW biosensor.

(Zhang et al., 2010). The SiNWs were formed in an array format through conventional optical lithography, etching and oxidation, and thus are fully compatible with CMOS technology. Fig. 1a shows optical image of the working SiNW chip and Fig. 1b illustrates SEM image of individual SiNW sensor. The nanowire chip for bio-sensing fabricated in the work is designed with 36 clusters of 5 nanowires each. The SiNW arrays are 90 μm in length and 2 μm spacing in between two wires. The typical resistance of the SiNW used for the work ranges from 10 to 25 MΩ.

Fig. 1c illustrates the working principle of the SiNW biosensors for studying the interactions of ER–ERE. ER is covalently immobilized on the electrically addressable SiNW surface via conventional silane chemistry. Electrical bio-sensing by SiNW is based on change in resistance of the SiNWs due to depletion of charge carriers in its "bulk" when the negatively charged ERE are bound to the ER-functionalized surface. When wt-ERE is applied to the immobilized ER, obvious resistance change occurs because wt-ERE is capable of recognizing the ER. Nonetheless, when non-ERE is used, resistance change is minimal as the non-ERE has the sequence in the ERE arms scrambled. In case of mut-ERE, the binding of mut-ERE and ER is not stable because of the mutation in each of the half-sites, so the resistance change is smaller compared to that obtained from the binding of wt-ERE and ER. As each wire is provided with independent metal contacts, resistance can be individually measured.

3.2. Fluorescence verification of binding of wt-ERE to ERα immobilized on the silicon substrate

To verify that ERE is capable of binding itself to the ER which is covalently immobilized on the SiNW surface, fluorescence imaging is used to illustrate binding of the immobilized ER with ERE on bare silicon substrate surface. To do so, a silicon substrate was treated with APTES and glutaraldehyde as aforementioned. 10 μl of ERα was manually spotted on the aldehyde-modified silicon surface. Amino-PEG was used to block the unreacted aldehyde groups on the surface. Then the ERα-spotted substrate was incubated with 10 μM wt-ERE labeled with a fluorescence tag in a humid atmosphere for 1 h. Wt-ERE containing forward sequence 5′-CAACTGGGTCATTCTGACCTAGAAG-3′ labeled with Cy 3 at its 5′-end and reverse sequence 5′-CTTCTAGGTCAGAATGACCCAGTTG-3′ was annealed in 6× SSC buffer solution. After washing, the binding event was finally imaged by fluorescence microscope. A spot was observed, illustrating that the wt-ERE was specifically bound to the spotted ERα (Figure S1). However, the fluorescent intensity inside the spot is not very strong probably because the native oxide-covered silicon substrate has high refractive index. In order to demonstrate that the fluorescent spot is caused by the interactions of ERα and wt-ERE, non-ERE labeled with the fluorescence tag is employed. Likewise, non-ERE containing forward sequence 5′-CAACTGATCGGTTCCTCGATAGAAG -3′ labeled with Cy 3 at its 5′-end and reverse sequence 5′-CTTCTATCGAGGAACCGATCAGTTG-3′ was annealed and incubated with the ERα-spotted silicon substrate for 1 h. Hardly any fluorescence spot was visible, indicating that the binding of ERα and non-ERE did not occur. The results show that binding of wt-ERE and ERα takes place, whereas no binding of non-ERE and ERα takes place as anticipated.

3.3. Interactions of ER with sequence-specific ERE

The three EREs are 25-bp long double-stranded oligonucleotides. The wt-ERE contains the palindromic GGTCA half-site with a 3-bp separation. The mut-ERE has a symmetric base mutation in each of ERE half-sites. The non-ERE has the sequence in the ERE arms scrambled. The sequence specificity was investigated by applying these three EREs to the ERα-functionalized SiNW, and the resistance change was shown in Fig. 2a. An obvious change (~26.0%) was seen when 1 pM wt-ERE was used, whereas only a negligible change (~1.9%) was obtained when 1 pM non-ERE was applied to the SiNW device. A smaller change (~8.9%) was observed when 1 pM mut-ERE was utilized. This is because the binding of mut-ERE to ERα is weaker than that of wt-ERE to ERα. These results demonstrate that the SiNW biosensor is capable of distinguishing the sequence specificity in consensus and mutant ERE.

Human ER has two subtypes, ERα and ERβ. To understand the interactions of various EREs with ERβ, the SiNW surface was first functionalized with ERβ, and the same concentrations of wt-ERE,

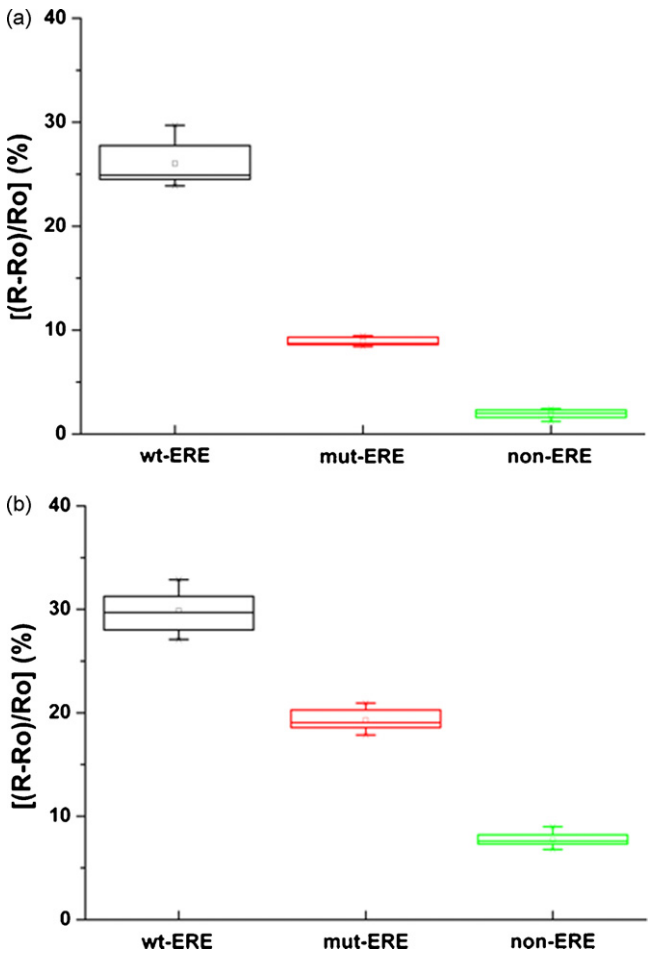

Fig. 2. Interactions of various EREs with ERα and ERβ immobilized on the SiNW surface. (a) Specificity of various EREs including wt-ERE, mut-ERE and non-ERE to the immobilized ERα. (b) Specificity of various EREs including wt-ERE, mut-ERE and non-ERE to the immobilized ERβ.

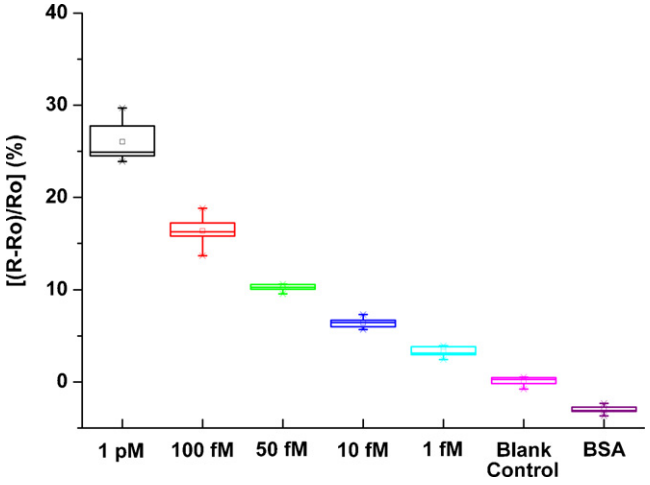

Fig. 3. Response of various concentrations of wt-ERE ranging from 1 pM to 1 fM to ERα functionalized on the SiNW surface. Blank control, in which no wt-ERE in the buffer was applied to the functionalized SiNW surface, showed negligible change in resistance. Likewise, another control, in which BSA was immobilized on the SiNW surface in place of ERα, also exhibited negligible change in resistance.

mut-ERE, and non-ERE were then applied to the ERβ-functionalized surface, respectively. As seen from Fig. 2b, the binding of ERβ–wt-ERE gave rise to a ~29.9% resistance increase, while the binding of ERβ–mut-ERE resulted in a ~19.3% resistance increase, and the binding of ERβ-non-ERE induced a ~7.7% resistance increase. Interestingly, the resistance changes of ERβ–ERE binding are higher than those of ERα–ERE binding. This is probably because ERα binds to ERE as a dimer, whereas ERβ binds to the ERE as tetramers.

The resistance changes caused by ERα–wt-ERE and ERβ–wt-ERE binding are higher than those obtained by ERα–mut-ERE and ERβ–mut-ERE binding, revealing that ERα and ERβ bind to the specific region (GGTCATTCTGACC) in the wt-ERE, whereas the binding is reduced by the base mutant ERE (G*T*TCATTCTGA*T*C). Furthermore, ERα shows a higher specificity than ERβ as the bindings of ERβ with mut-ERE and non-ERE, respectively, cause a bigger change in resistance, which implies difficulty in distinguishing sequence. The results are in good agreement with those obtained by the SPR-based methodology for studying ER–ERE interactions (Su et al., 2006).

3.4. Sensitivity of ERα–wt-ERE binding

SiNWs serve as a highly sensitive and label-free sensor with unique sensing principle due to its large surface-to-volume ratio and tunable electrical properties. High sensitivity of the SiNW biosensor has been established in nucleic acid and protein detection, however much is unknown about how sensitive protein interacts with DNA with the SiNW biosensor. Hence, this study serves to substantiate of SiNW sensitivity by monitoring the resistance change caused by the binding of wt-ERE to ERα. Fig. 3 portrays the response of various concentrations of wt-ERE, ranging from 1 fM to 1 pM, bound to the immobilized ERα. A descending trend (~26.0% for 1 pM wt-ERE, ~16.3% for 100 fM wt-ERE, ~6.4% for 10 fM wt-ERE, and ~3.3% for 1 fM wt-ERE, respectively) could be observed for decreasing concentrations of wt-ERE. A negligible response was observed when a buffer solution without wt-ERE was added to the ERα-functionalized surface. To verify the binding specificity between ERα and wt-ERE, another control experiment was carried out, in which the wt-ERE was applied to the SiNW surface functionalized with BSA. Hardly any resistance change was visible, showing that the wt-ERE did not bind the unspecific protein. Based on the signal-to-noise ratio obtained from the ERα–ERE binding, limit of detection for the binding of ERα–ERE is 10 fM. The high sensitivity that the SiNW biosensor can particularly confer facilitates the studies on binding affinity between ER and ERE.

3.5. Effect of salt concentrations on ER–ERE binding

Understanding how salt concentration affects ER–ERE interactions could provide an insight into the mechanism of ER questing for a specific ERE sequence. It was reported that ER–ERE interactions were certainly affected by the salt concentrations. SPR experiments showed that the high salt concentrations reduced the ER binding to the EREs (Su et al., 2006). To demonstrate the effect of salt concentrations on ER–ERE binding with the SiNW biosensor, 1 pM wt-ERE in various concentrations of buffer solutions ranging from 10× SSC to 0.01× SSC was incubated with the ERα-modified SiNW surface, and the response was obtained by measuring the resistance change before and after the binding of wt-ERE to the immobilized ERα in 0.01× SSC solution. Fig. 4 shows varying response versus different buffer solution used for ERα–wt-ERE binding. Results show that a decreased salt concentration from 6× SSC to 0.01× SSC disrupts the DNA binding to the protein, meanwhile an increased salt concentration from 6× SSC to 10× SSC also interrupts the binding. The pH of the buffer solution used is 7.0, so ERα (p*I*: ~8.3) is positively charged and on the contrary DNA is negatively charged. The formation of protein–DNA is mainly dependent on three factors, electrostatic, hydrogen bond and van der Waals force. At a

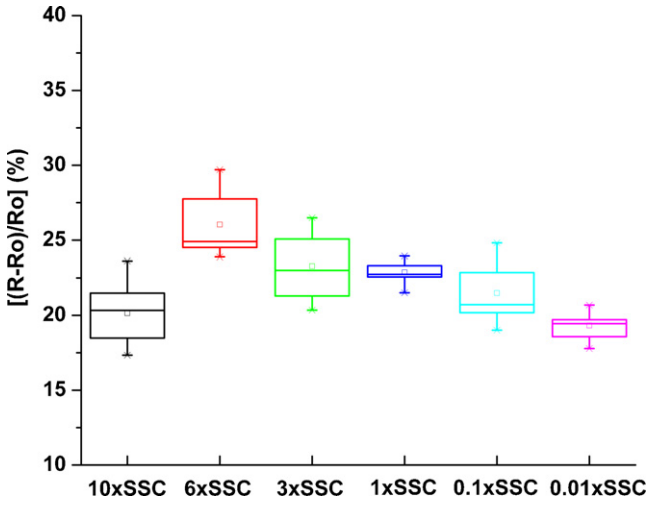

Fig. 4. Response of the SiNW biosensor versus varying salt concentrations of buffer solution for the incubation of 1 pM wt-ERE with the immobilized ERα. The measuring buffer is 0.01× SSC.

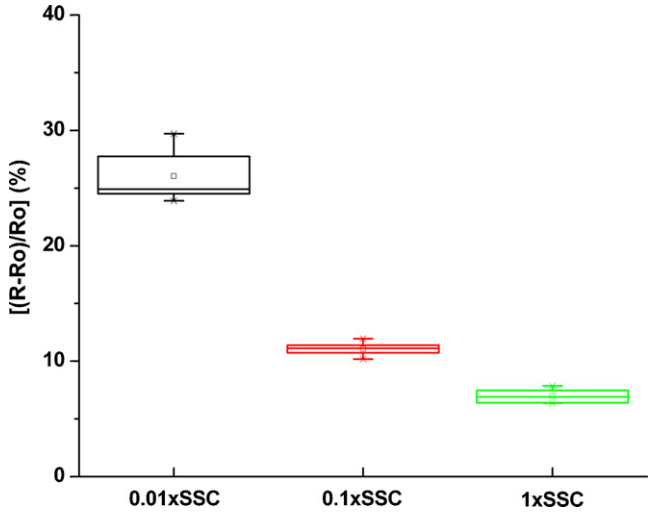

Fig. 5. Response of the SiNW biosensor versus varying ionic strengths of buffer solutions for measurements. 1 pM wt-ERE in 6× SSC was interacted with ERα functionalized on the SiNW surface prior to measurement.

higher ionic strength, the interactions are mainly disturbed by the salt ions competing with DNA for the electrostatic binding to protein. As a result, the increased salt concentrations from 6× SSC to 10× SSC depleted wt-ERE binding by ~22.7% to ERα. In the case of a lower ionic strength, the protein–DNA complex is primarily formed through hydrogen bond and van der Waals force. As the salt concentrations decrease, the hydrogen bond and van der Waals force play a weaker role in binding, thus depleting the interactions. As shown in Fig. 4, the decreased salt concentration from 6× SSC to 0.01× SSC depleted wt-ERE binding by ~25.7% to ERα.

3.6. Influence of ionic strength of measuring buffer on detection sensitivity

The importance of the Debye length on nanowire field effect transistor sensors has been extensively reported (Chua et al., 2009; Stern et al., 2007b). The Debye length can be estimated by calculation using the formula: $\lambda_D = 0.32(I)^{-0.5}$, where I is the ionic strength of the buffer solution used for measurement. In other words, the Debye length is inversely proportional to ionic strength. A low ionic strength ensures that the Debye length is larger and the screening of charges is less, thereby increasing the detection sensitivity. To study the effect of different SSC buffer solution on detection sensitivity, 1 pM wt-ERE in 6× SSC was bound to the ERα-functionalized SiNWs sensor and the measurements were carried out in three different SSC buffer solution, 1× SSC, 0.1× SSC and 0.01× SSC, respectively, before and after binding of wt-ERE with ERα. The ionic strength of 0.01× SSC is 1.65 mM, corresponding to a Debye length of approximately 8.0 nm. Likewise, the ionic strength of 0.1× SSC and 1× SSC result in Debye length of about 2.5 nm and 0.8 nm, respectively. As seen in Fig. 5, approximately 26.0% increase in resistance response was observed when the measurement was conducted in 0.01× SSC solution, indicating that the majority of the bound DNA's negative charges is unscreened. A 10-fold increase in the ionic strength of the buffer from 0.01× SSC to 0.1× SSC gave rise to a ~11.1% increase in resistance response because the decreasing Debye length partially screened DNA's intrinsic negative charges. A further 10-fold increase in buffer ionic strength from 0.1× SSC to 1× SSC effectively screened most of DNA's negative charges, causing only a ~7.0% resistance increase. It is demonstrated that the increasing measuring buffer ionic strength reduces the detection sensitivity for ERα–wt-ERE binding.

3.7. Regeneration of the ERα-functionalized SiNW sensor

To investigate the regeneration of the ERα-functionalized SiNW sensor, real-time monitoring of ER–ERE binding was conducted. Figure S2 records the conductance change as a function of time when the wt-ERE is bound to the ERα on the SiNW surface. As observed, the conductance dropped dramatically upon addition of 1 nM wt-ERE in 0.01× SSC, which corresponds to the increase in resistance. The results are consistent with those in Fig. 3. It was reported that 0.1% SDS could be used to dissociate the protein–DNA binding (Su et al., 2006). The baseline was restored after the ERα-functionalized SiNW sensor was exposed to 0.1% SDS solution for 5 min, followed by the addition of the measuring buffer (0.01× SSC) again, indicating that the wt-ERE was detached from the SiNW surface by SDS. Further addition of 1 nM wt-ERE resulted in a smaller drop in conductance. The baseline was restored again by re-treating the sensor with 0.1% SDS and SSC buffer. However, no more change in conductance was obtained upon addition of the same concentration of wt-ERE. The results suggest that the ERα-functionalized SiNW sensor can be regenerated once for ERE binding. This unique capability allows the sensitive SiNW biosensor to work as a reusable device for rapid screening of estrogen-mediated gene expression.

4. Conclusions

The SiNW bio-sensing scheme of applying ER as a capture probe to interact with ERE is different from many of the previously reported approaches that used ERE as a probe to characterize ER–ERE binding. In this paper, we demonstrated the capabilities of the ER-functionalized SiNW biosensor for the identification of the various EREs including wt-ERE, mut-ERE and non-ERE. The ERα-functionalized SiNW biosensor allows for a sensitive determination of wt-ERE as high as 10 fM, as well as a comprehensive understanding on specificity between ERs and various EREs. Furthermore, the SiNW biosensor is reusable for studying protein–DNA interactions.

In most cases, our findings are in good agreement with those found by other methods (Su et al., 2006). However, the SiNW biosensor impressively illustrates a very low concentration of wt-ERE, down to femtomolar, can be bound to the immobilized ERα, which is an extremely obvious differentiator from other technologies. The silicon nanowire biosensor not only provides an alternative method, but also establishes a highly sensitive and new solution to study the ER–DNA interactions. It is believed that the

developed SiNW biosensor will benefit the studies in hormone receptor biology to rapidly and sensitively screen the binding sites of estrogen-responsive genes with the receptors.

Acknowledgment

The authors would like to acknowledge The Agency for Science, Technology and Research (A*STAR), Singapore, for the financial support under the Grant CCOG01-005-2008.

Appendix A. Supplementary data

Supplementary data associated with this article can be found, in the online version, at doi:10.1016/j.bios.2010.07.129.

References

Bunimovich, Y.L., Shin, Y.S., Yeo, W.-S., Amori, M., Kwong, G., Heath, J.R., 2006. J. Am. Chem. Soc. 128, 16323–16331.
Cheskis, B.J., Karathanasis, S., Lyttle, C.R., 1997. J. Biol. Chem. 272, 11384–11391.
Chua, J., Chee, R.E., Agarwal, A., Wong, S.M., Zhang, G.-J., 2009. Anal. Chem. 81, 6266–6271.
Cui, Y., Wei, Q.Q., Park, H.K., Lieber, C.M., 2001. Science 293, 1289–1292.
Driscoll, M.D., Klinge, C.M., Hilf, R., Bambara, R.A., 1996. J. Steroid Biochem. Mol. Biol. 58, 45–61.
Evans, R.M., 1988. Science 240, 889–895.
Gao, Z.-Q., Agarwal, A., Trigg, A.D., Singh, N., Fang, C., Tung, C.-H., Fan, Y., Buddharaju, K.D., Kong, J.-M., 2007. Anal. Chem. 79, 3291–3297.
Hahm, J.-I., Lieber, C.M., 2004. Nano Lett. 4, 51–54.
Klein-Hitpass, L., Schorpp, M., Wagner, U., Ryffel, G.U., 1986. Cell 46, 1053–1061.
Klein-Hitpass, L., Ryffel, G.U., Heitlinger, E., Cato, A.C.B., 1988. Nucleic Acids Res. 16, 647–663.
Li, Z., Chen, Y., Li, X., Kamins, T.I., Nauka, K., Williams, R.S., 2004. Nano Lett. 4, 245–247.
Lin, T.-W., Hsieh, P.-J., Lin, C.-L., Fang, Y.-Y., Yang, J.-X., Tsai, C.-C., Chiang, P.-L., Pan, C.-Y., Chen, Y.-T., 2010. Proc. Natl. Acad. Sci. U. S. A. 107, 1047–1052.
Loven, M.A., Wood, J.R., Nardulli, A.M., 2001. Mol. Cell Endocrinol. 181, 151–163.
Lyubchenko, Y.L., Shlyakhtenko, L.S., 2009. Methods 47, 206–213.
Moras, D., Gronemeyer, H., 1998. Curr. Opin. Cell Biol. 10, 384–391.
Ozers, M.S., Hill, J.J., Ervin, K., Wood, J.R., Nardulli, A.M., Royer, C.A., Gorski, J., 1997. J. Biol. Chem. 272, 30405–30411.
Stern, E., Klemic, J.F., Routenberg, D.A., Wyremebak, P.N., Turner-Evans, D.B., Hamilton, A.D., LaVan, D.A., Fahmy, T.M., Reed, M.A., 2007a. Nature 445, 519–522.
Stern, E., Wagner, R., Sigworth, F.J., Breaker, R., Fahmy, T.M., Reed, M.A., 2007b. Nano Lett. 7, 3405–3409.
Su, X.D., Lin, C.Y., O'Shea, S.J., Teh, H.F., Peh, W.Y.X., Thomsen, J.S., 2006. Anal. Chem. 78, 5552–5558.
Teh, H.F., Peh, W.Y.X., Su, X.D., Thomsen, J.S., 2007. Biochemistry 46, 2127–2135.
Wicaksono, D.H.B., Ebihara, T., Funabashi, H., Mie, M., Yanagida, Y., Aizawa, M., Kobatake, E., 2004. Biosens. Bioelectron. 19, 1573–1579.
Yi, P., Driscoll, M.D., Huang, J., Bhagat, S., Hilf, R., Bambara, R.A., Muyan, M., 2002. Mol. Endocrinol. 16, 674–693.
Zhang, G.-J., Chua, J., Chee, R.E., Agarwal, A., Wong, S.M., 2009. Biosens. Bioelectron. 24, 2504–2508.
Zhang, G.-J., Chua, J., Chee, R.E., Agarwal, A., Wong, S.M., Buddharaju, K.D., Balasubramanian, N., 2008a. Biosens. Bioelectron. 23, 1701–1707.
Zhang, G.-J., Zhang, G., Chua, J., Chee, R.E., Wong, E.H., Agarwal, A., Buddharaju, K.D., Singh, N., Gao, Z.Q., Balasubramanian, N., 2008b. Nano Lett. 8, 1066–1070.
Zhang, G.-J., Zhang, L., Huang, M.J., Luo, Z.H.H., Tay, G.K.I., Lim, E.-J.A., Kang, T.G., Chen, Y., 2010. Sens. Actuators B: Chem. 146, 138–144.
Zheng, G., Patolsky, F., Cui, Y., Wang, W.U., Lieber, C.M., 2005. Nat. Biotechnol. 23, 1294–1301.